

# Sonochemical Deposition of Silver Nanoparticles on Wool Fibers

Liraz Hadad,<sup>1</sup> Nina Perkas,<sup>1</sup> Yosef Gofer,<sup>1</sup> Jose Calderon-Moreno,<sup>2</sup> Anil Ghule,<sup>3</sup> Aharon Gedanken<sup>1</sup>

<sup>1</sup>Department of Chemistry and Kanbar Laboratory for Nanomaterials, Center for Advanced Materials and Nanotechnology, Bar-Ilan University, Ramat-Gan 52900, Israel

<sup>2</sup>Applied Physics Department, Universitat Politècnica de Catalunya, Avenida Canal Olímpic, Castelldefels, 08860 Barcelona, Spain

<sup>3</sup>Department of Chemistry, National Tsing Hua University, 2 Kuang Fu Road, Hsin Chu, Taiwan

Received 5 July 2006; accepted 30 October 2006

DOI 10.1002/app.25813

Published online in Wiley InterScience (www.interscience.wiley.com).

**ABSTRACT:** Silver nanoparticles were deposited on the surface of natural wool with the aid of powered ultrasound. The average particle size was 5–10 nm, but larger aggregates of 50–100 nm were also observed. The sonochemical irradiation of a slurry containing wool fibers, silver nitrate, and ammonia in an aqueous medium for 120 min under an argon atmosphere yielded a silver–wool nanocomposite. By varying the gas and reaction conditions, we could achieve control over the deposition of the metallic silver particles on the surface of the wool fibers. The resulting silver-deposited wool samples were characterized with X-ray diffraction, transmission electron microscopy, high-resolution transmission electron microscopy, high-re-

solution scanning electron microscopy, electron-dispersive X-ray analysis, Brunauer, Emmett, and Teller physical adsorption method, X-ray photoelectron spectroscopy, and Raman and diffused reflection optical spectroscopy. The results showed that the strong adhesion of the silver to the wool was a result of the adsorption and interaction of silver with sulfur moieties related to the cysteine group. © 2007 Wiley Periodicals, Inc. *J Appl Polym Sci* 104: 1732–1737, 2007

**Key words:** fibers; irradiation; metal-polymer complexes; nanocomposites; nanolayers; nanoparticles; proteins

## INTRODUCTION

The growing interest in textile materials with antimicrobial properties has stimulated an extensive search for new technologies for the modification of wool fibers and the production of safety yarns.<sup>1–3</sup> Different types of antimicrobial treatments have been studied for the protection of wool products from damage caused by pathogenic microorganisms. Among these treatments, there is the coating of wool with resin-bonded copper-8-quinolinolate, chlorinated phenol and its derivatives, sodium dichloroisocyanurate, quaternary ammonium compounds, metal ions, and organic tin compounds in finishing processes.<sup>4–6</sup> A novel biotemplate redox technique has been employed for the deposition of silver nanoclusters on another type of natural fiber—silk fibroin fiber.<sup>7</sup>

Wool fibers as proteins consist of polar groups of amino acid residues able to bind other charged organic and inorganic molecules. The cationic amine salts can interact with anionic acidic groups in acid dyes to form ionic pairs, thus coloring the wool fibers.

Similarly, the carboxylic acid groups existing in wool proteins are also interactive with many other cationic compounds. For instance, metal ions such as Ag<sup>+</sup> and Cu<sup>2+</sup> can be absorbed into the wool fibers.<sup>7,8</sup> It has been demonstrated that the treatment of wool with metal nanoparticles may induce useful changes in natural fibers such as antistatic properties, electrical conductivity, and antimicrobial activity.<sup>9,10</sup>

The principal requirements for metal–fiber nanocomposites are small dimensions, regular shapes, and uniform size distributions of the silver nanoparticles. Sonochemical irradiation has been proven to be an effective method for the synthesis of nanophase materials and for the deposition and insertion of nanoparticles onto and into mesoporous and ceramic supports as well as polymers. The efficiency of sonochemistry comes from the explosive collapse of the bubbles forming in the liquid as a result of sonochemical irradiation. The hot-spot mechanism explains that the effect of very high temperatures obtained upon the collapse of the bubbles, following by very high cooling rates, leads to the creation of nanostructure products.<sup>11,12</sup> The advantage of this method, which has been demonstrated, is the achievement of a very homogeneous coating with a narrow particle size distribution.<sup>13,14</sup> In previous publications, we have reported the preparation of amorphous silver about 20 nm in

Correspondence to: A. Gedanken (gedanken@mail.biu.ac.il).

size<sup>15</sup> and the deposition of homogeneously distributed silver nanoparticles with an average diameter of  $\sim 5$  nm on the surface of silica submicrospheres with the aid of ultrasound irradiation.<sup>16</sup> In this report, we for first time present the results of the one-stage sonochemical deposition of silver nanoparticles on wool protein fibers and their characterization with a series of physicochemical methods.

## EXPERIMENTAL

### Materials

White merino wool fibers were used without further purification. The chemicals (chemically pure grade) were purchased from Sigma–Aldrich (Steinheim, Germany). The deposition of silver on the wool fibers was performed by ultrasound irradiation; namely, 0.8 g of wool fibers and 0.17 g of silver nitrate (corresponding to a 0.004M solution of AgNO<sub>3</sub>) were added to 230 mL of distilled water and 20 mL of ethylene glycol in a 300-mL sonication cell. The cell was attached to the sonicator under a flow of argon. Argon gas was bubbled through the slurry before sonication to remove the dissolved oxygen/air. This reaction was also conducted with the same reagent composition under a flow of an argon/hydrogen gas mixture (95 : 5; samples 1 and 2). The gas, Ar/H<sub>2</sub>, was bubbled for 1 h before sonication for sample 1 and for 24 h before sonication for sample 2. For sample 3, argon was bubbled for 24 h before sonication. The ultrasound irradiation of the slurry was performed for 2 h by the direct immersion of a high-intensity titanium horn (VCX 600 sonifier, Sonics and Materials (Newtown, CT); 20 kHz, 40 W/cm<sup>2</sup>) in a sonication cell under an argon flow; 0.5 mL of 24 wt % aqueous ammonia was added dropwise during the sonication. A sonication cell was placed in a bath filled with ice water, and a temperature of 15–20°C was maintained during the sonication. The product was washed thoroughly with 500 mL of distilled water and then with 250 mL of ethanol under the inert atmosphere of a glovebox and dried in a vacuum of 10<sup>-2</sup> mmHg overnight. A control sonochemical reaction with identical conditions and concentrations of the reagents was carried out in the absence of AgNO<sub>3</sub>. No morphological changes or modifications in the characteristic surface parameters were detected in the various measurements.

### Measurements

X-ray diffraction (XRD) studies were carried out with a Bruker D8 diffractometer (Karlsruhe, Germany) with Cu K $\alpha$  radiation. The morphology of the particles and the nature of their adherence to wool were studied with transmission electron microscopy (TEM) on a JEOL JEM 100 SX microscope (Tokyo, Japan) working at a 100-kV accelerating voltage. High-resolution trans-

mission electron microscopy (HRTEM) images were obtained with a JEOL 3010 microscope set to a 300-kV accelerating voltage. High-resolution scanning electron microscopy (HRSEM) images were performed with a Leo Gemini 982 field emission gun scanning electron microscope (Oberkochen, Germany) operating at a 4-kV accelerating voltage.

The silver content in the wool fibers was determined by volumetric titration with KSCN according to the Foldgard method after the dissolution of the material in HNO<sub>3</sub>.<sup>17</sup> The elemental composition of the material was also analyzed with electron-dispersive X-ray (EDX) analysis on a JEOL JSM 840 scanning electron microscope. The surface was measured with a Micromeritics Gemini 2375 analyzer after the samples were heated at 120°C for 1 h. The specific surface area was calculated from the linear part of the BET plot at 196°C. The energy state of silver was determined by X-ray photoelectron spectroscopy (XPS) on a Kratos Axis HS spectrometer (Manchester, UK) with Al K $\alpha$  radiation. The C1s with binding energy ( $E_b = 285.0$  eV) was chosen as a reference line for the calibration of the energy scale. The spectroscopy studies were also performed with infrared spectroscopy, diffusion reflection, and Raman methods. The diffused reflection optical spectra were recorded on a Cary 100 Scan UV spectrometer (Melbourne, Australia) in the wavelength range of 200–600 nm. The Raman spectra were collected with a JY Horiba Olympus Bx41 spectrometer (Longjumeau, France) with a 514-nm laser excitation source.

## RESULTS AND DISCUSSION

### Influence of the experimental conditions on the silver content in the wool fibers

The sonochemical irradiation of wool fibers in an aqueous solution of silver nitrate containing ethylene glycol under a reducing atmosphere of an argon/hydrogen gas mixture (95 : 5) resulted in the coating of the neat wool fibers with silver nanoparticles. However, larger aggregates were also observed. The concentration of silver and the specific surface area of the coated wool fibers depended on the reaction conditions. The specific surface area of the neat wool fibers was about 1 m<sup>2</sup>/g, and it increased almost to 4.6 m<sup>2</sup>/g because of the incorporation of the silver nanoparticles. The nanoparticles generally demonstrated a significant surface area because the ratio of the surface to the volume of the materials grew with a reduction of the particle size. The reason that the gaseous atmosphere under which sonication was conducted was varied was to clarify whether the H<sub>2</sub>/Ar mixture served as the reducing agent. The results presented in Table I show that the reducing agent was clearly ethylene glycol. This was deduced from the reduction of sample 3, for which sonication conducted under Ar

**TABLE I**  
Experimental Conditions for the Preparation of the Samples

Sample	Bubbling duration	Silver (% w/w)		Specific surface area (m <sup>2</sup> /g)
		Volume titration	EDX	
Neat wool	—	—	—	1.0 ± 0.1
1	1 h, Ar/H <sub>2</sub>	0.6 ± 0.1	0.9 ± 0.1	2.3 ± 0.2
2	24 h, Ar/H <sub>2</sub>	3.7 ± 0.3	4.1 ± 0.2	3.9 ± 0.4
3	24 h, Ar	6.9 ± 0.4	7.2 ± 0.3	4.6 ± 0.5

yielded the highest amount of silver on the wool fibers, as well as the highest surface area. The reason that argon was a better reducing environment than the H<sub>2</sub>/Ar mixture in samples 1 and 2 has to do with the lowering of the maximum temperature obtained upon the collapse of the cavitation bubble under a monoatomic gas, rather than when a diatomic gas was present. The silver concentrations of the studied samples were measured with the EDX technique. They did not differ from those obtained by chemical titration (Table I). The silver concentrations measured with EDX were slightly higher, probably because the EDX technique could probe a depth of only up to 600–

1000 nm, whereas titration monitored the total content of silver.

### Electron microscopy studies

A TEM image of silver-coated wool is shown in Figure 1(b), and a TEM micrograph of the neat wool fibers is presented for comparison in Figure 1(a). The particle size distribution was calculated with the Scion program. A histogram (Fig. 2) shows that most of the deposited particles (ca. 50%) were in the range of 5–10 nm with a standard deviation of 1 nm. Some balls observed in the photograph [Fig. 1(b)] were related to heaps of wool fibers.

The HRTEM micrograph demonstrates an isolated wool fiber coated with silver nanoparticles [Fig. 3(a)]. The separate silver nanoparticles were well distinguished on the surface of the wool fibers. HRTEM has been also used to study the nature of the individual small nanoparticles on the wool's surface. In the micrographs of sample 3 shown in Figure 3(b), we can clearly see that the shape of the nanoparticles was close to spherical. Fringes can be clearly observed in the images and help with their characterization as a cubic lattice of metallic silver (powder diffraction files database (PDF): 4-783). The distance between the lattice planes was equal to 0.239 nm, which was very close to the spacing between the [111] planes in the corresponding face-centered cubic silver structure

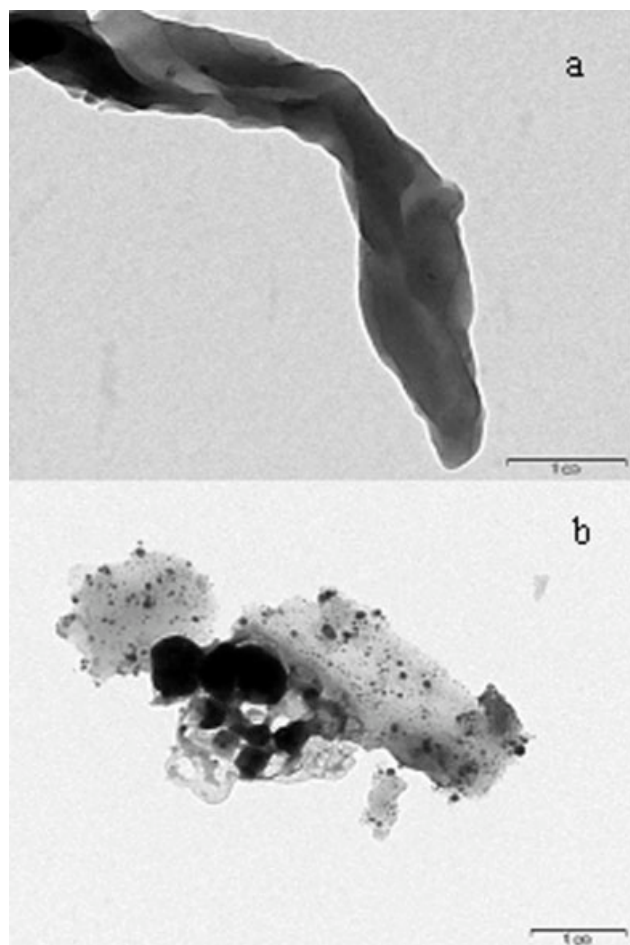


**Figure 1** TEM images of (a) neat and (b) silver-coated wool fibers (sample 3; scale bar = 1 μm).

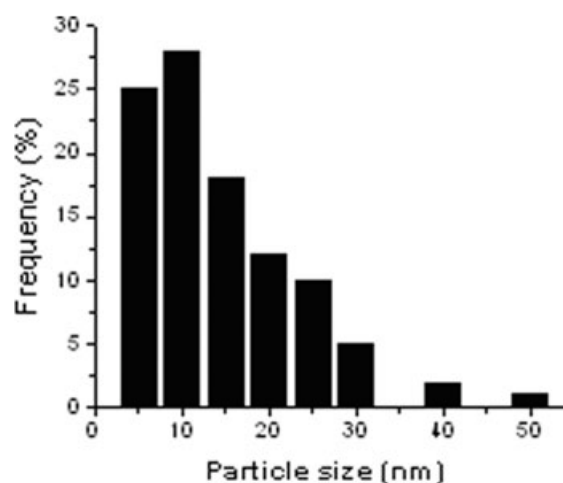


**Figure 2** Histogram of TEM images of sample 3.

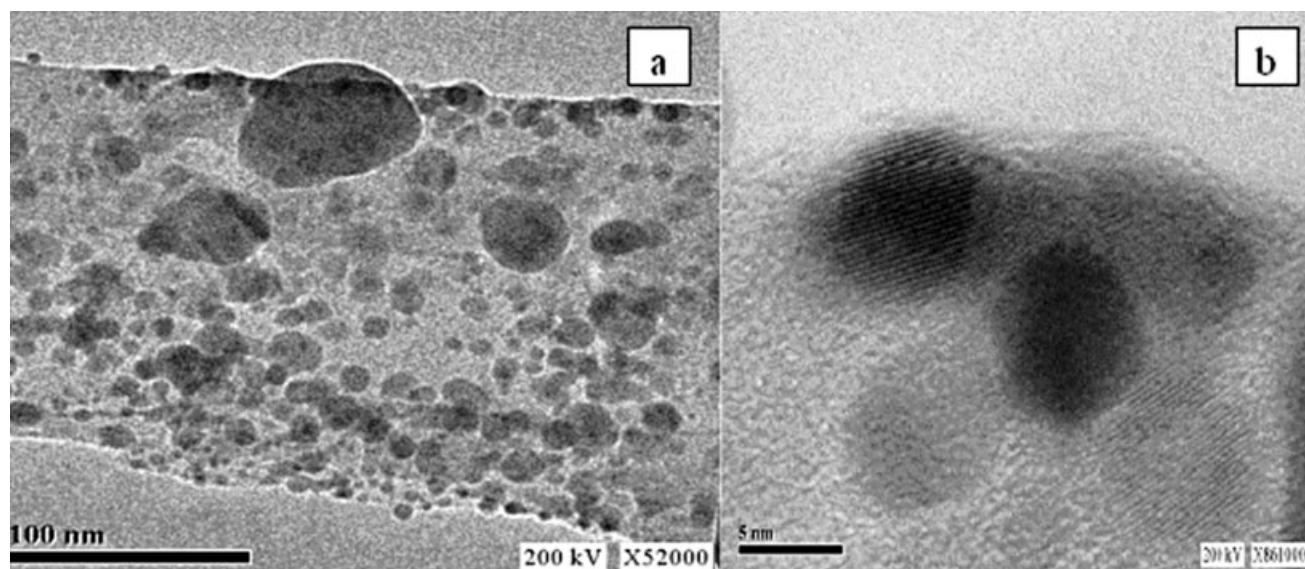


**Figure 3** HRTEM images of silver-coated wool fibers (sample 3): (a) fiber image (scale bar = 100 nm) and (b) individual particles on the surface of the wool fiber (scale bar = 5 nm).

(0.236 nm). No oxide layer was observed on the surface of these nanoparticles (more than 20 particles were examined). The XRD studies of all the prepared samples did not reveal the crystalline structure. This is explained as the result of the small size of the particles, which caused a severe broadening of the diffraction pattern and smeared out the corresponding diffraction peaks. In a previous case,<sup>16</sup> we explained the absence of an XRD pattern as due to the amorphous nature of the silver. However, the lack of XRD in this case and the clear detection of silver fringes in HRTEM indicate that we were wrong in ref. 16 and that the material was rather X-ray amorphous. The same is true in this case; namely, the silver was nano-

crystalline, but X-ray amorphous, because of the small particle size.

The morphology of the wool fibers has been examined by means of HRSEM analysis. An image of the neat wool fiber is shown in Figure 4(a). The typical scaled structure of a wool fiber can be observed. It consists of cuticle cells overlapping to form a structure like that of tiles on a roof.<sup>18</sup> The picture shows a high extent of heterogeneity of the surface coating; namely, certain areas are densely coated, whereas in others, a sparsely coated pattern can be observed.

In Figure 4(b), we can see changes in the wool fibers after sonication with silver nitrate. There were silver clusters on the surface of the wool fibers about 50 nm

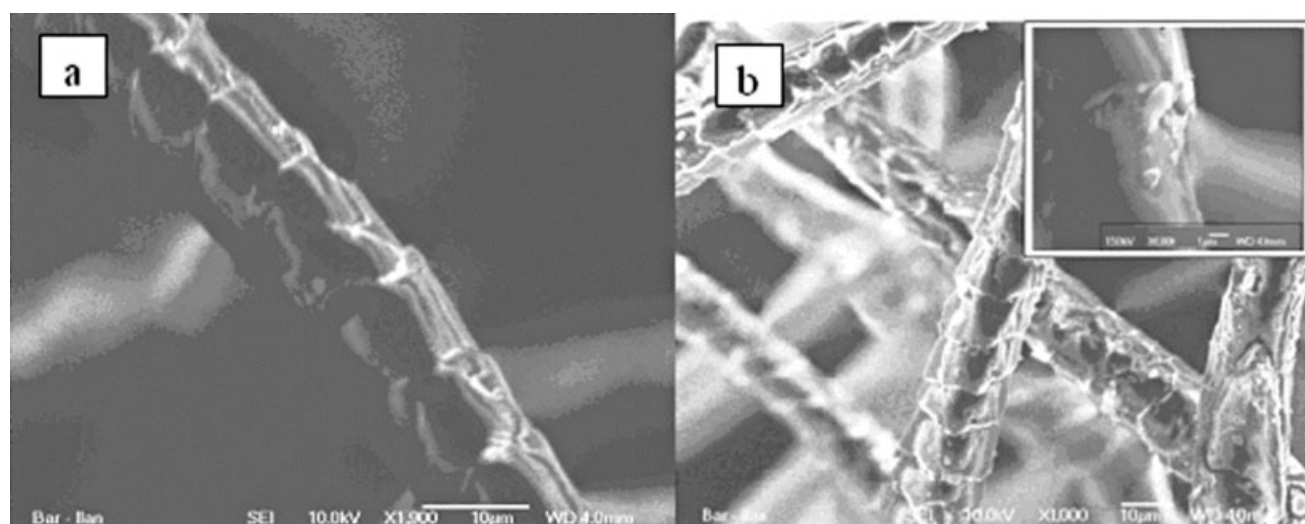


**Figure 4** HRSEM images of (a) neat wool fibers (scale bar = 10 μm) and (b) wool fibers coated with silver [the inset shows a high-magnification image (6000×) of the selected area].



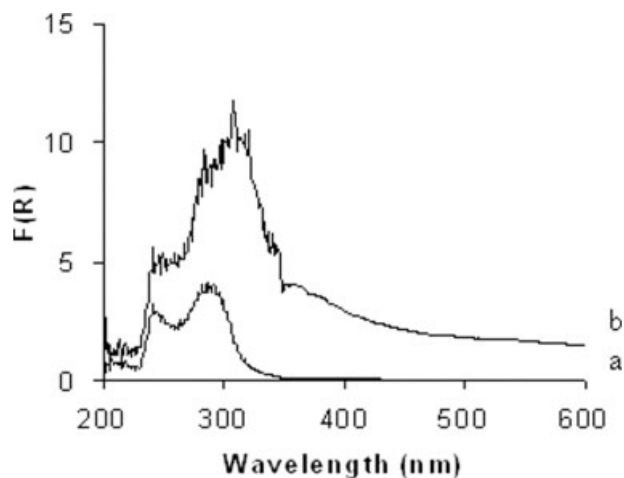


**Figure 5** Diffused reflection optical spectra of (a) neat and (b) silver-coated wool fibers.  $F(R)$  is an optical correlation function between a target and the reference sample.

in size. Some of them were well separated, but larger aggregates can also be observed. The HRTEM image (Fig. 3) demonstrates very clearly that each aggregate was composed of small nanoparticles. From the inserted picture in the upper right corner, it is clear that the deposition of nanoparticles mainly took place between the fiber crossovers.

### Spectroscopy studies

The diffused reflection optical spectra of the neat wool fibers demonstrate two bands at wavelengths of 250 and 285 nm (Fig. 5). After the sonochemical deposition of the silver on the wool, the intensity of these two bands increased, and an additional peak at about 325 nm could be observed in the spectrum. Its position is very different from the characteristic band at 400 nm of  $Ag(0)$  observed for colloid silver<sup>19</sup> or silver-poly vinyl pyrrolidone composites.<sup>20</sup> We assign this large

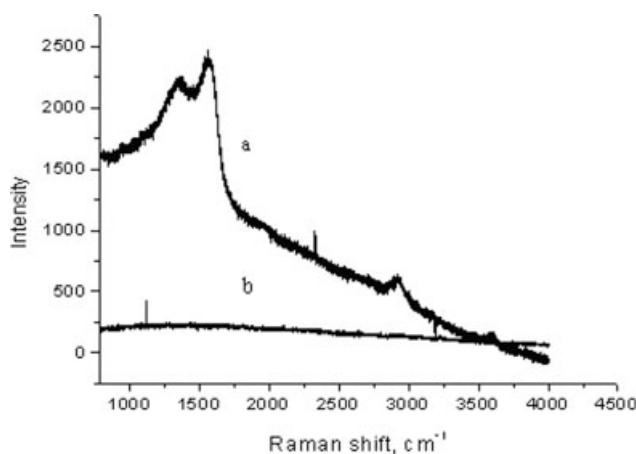


**Figure 6** Raman spectra of (a) neat and (b) silver-coated wool fibers.

blueshift to the interaction of the very small silver nanoparticles with the wool polymer.

In the Raman spectra (Fig. 6), we can clearly see two characteristic scattering peaks of zero-valence silver at 1300 and 1500  $cm^{-1}$ . These two Raman peaks have also been detected for pristine silver nanoclusters.<sup>21</sup> In the neat wool spectrum, we could not observe any discrete Raman scattering peaks.

### XPS

We washed the silver-coated fibers and saw that the silver was strongly bonded to the fibers and was not washed off, even after repeated washing cycles. This led us to investigate the nature of the interaction and bonding of the silver particles and the wool substrate. This was accomplished with XPS measurements. All the measurements were carried out on the neat and coated fibers. In the XPS spectra of C1s and O1s, no changes were found. This meant that neither carbon nor oxygen was directly involved in the interaction with the silver nanoparticles. Figure 7 shows the XPS spectra of S2p of neat wool and silver-coated wool fibers. The S2p photoemission spectra of sulfur in the neat wool were resolved into two peaks at 165.1 and 163.8 eV, corresponding to the value of S(2-).<sup>22</sup> For the silver-coated fibers, the S2p energy spectra of sulfur were shifted to lower energies and were resolved into three peaks at 164.2, 162.9, and 161.7 eV. The higher two energy peaks were similar to those of the neat wool fibers, and the third XPS band (at the lower energy) was attributed to the interaction between the sulfur atoms and silver nanoparticles. The new lower energy peak at 161.7 eV was attributed to sulfur atoms in the silver-coated fibers having a larger electronic density than those in the neat wool fibers. The 161.7-eV band resulted from the disconnection of the S—S bond in the keratin fibers. The dis-

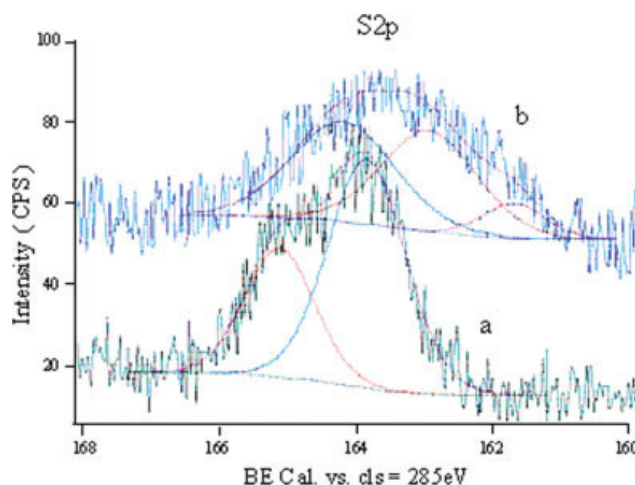


**Figure 7** XPS spectra of (a) neat and (b) silver-coated wool fibers. [Color figure can be viewed in the online issue, which is available at [www.interscience.wiley.com](http://www.interscience.wiley.com).]

connection of the S—S bond under reducing conditions was previously observed, especially in the cortex region.<sup>23</sup> Whether electrostatic interactions, the ionic bonds that were formed, or the reduced metallic silver atoms interacted with the electron-rich sulfur atoms is not clear. XPS just points out the location of the interaction of the silver but does not provide enough information for the nature of the bonding. We also conducted secondary-ion mass spectrometry time-of-flight measurements. We expected to determine if the silver removed from the surface carried into the gas phase either a whole cystein molecule or just a fracture of this molecule. However, only silver atoms were detected in the gas phase by the mass spectrometer.

The coating of nanoparticles on spherical surfaces of polymers and ceramic bodies by ultrasound radiation has been demonstrated in the past.<sup>16,24</sup> Current research extends this method to include polymeric protein fibers. The chemical reactions, driven by intense ultrasonic waves, lead to the formation of nanoparticles. These sonochemical reactions appear to occur within the interfacial region in the vicinity of solid materials.

It has already been demonstrated that the number of collapsing bubbles is enhanced under such circumstances in comparison with the same reaction in the absence of solid bodies. The advantage of the sonochemical method is that the production and deposition of nanosized powders on the surface of a solid substrate take place simultaneously. Moreover, one of the aftereffects of the collapsing bubble is the creation of microjets and shockwaves. The microjets throw the newly formed nanoparticles at the solid surfaces at such a high speed that they can melt, in the case of polymers, the solid surface and cause the deep penetration of the nanoparticles into the solid body. The mechanism by which the silver nanoparticles in our case are bonded to the wool surface is related to these microjets and shock waves.<sup>12</sup> The nanoparticles are anchored to the wool fibers by the formation of bonds or interactions between the silver and sulfur moiety of the cystein amino acid. This strong interaction prevents the removal of the silver nanoparticles by thermal washing. As a result, a stable, homogeneous coating is formed on the surface.

## CONCLUSIONS

In this work, we have demonstrated the deposition of small silver nanoparticles on wool fabrics by the coating of neat fibers with silver nanoparticles via ultrasound irradiation. We suggest that this product can serve as an antimicrobial fabric. The process is performed in a one-step sonochemical procedure with a

slurry-containing wool fibers, silver nitrate, and ammonia in an aqueous medium. The best coating was obtained when the bubbling of argon for 24 h preceded the sonication. The produced silver-coated wool fabrics maintained the high flexibility and elasticity typical of wool. The studies of the silver-coated wool fibers by physical and chemical methods have demonstrated the presence of highly dispersed silver nanoparticles (~ 5 nm) incorporated into the natural wool. Some of the silver particles aggregate into clusters located at the fiber crossovers. XPS studies have demonstrated that silver nanoparticles are attached to the keratin fibers as a result of the interaction between either Ag<sup>+1</sup> or Ag clusters and sulfur. The origin of these sulfur atoms is most likely the partial disconnection of the S—S bond in the keratin fibers. The stability of the coating is satisfactory: even after several cycles of thermal treatments and simulating laundering, no change in the silver concentration was detected.

## References

1. Sun, Y.; Sun, G. *J Appl Polym Sci* 2002, 84, 1592.
2. Kim, Y. H.; Sun, G. *Text Res J* 2002, 72, 1052.
3. Takasima, M.; Shirai, F.; Sageshima, M.; Ikeda, M.; Okamoto, Y.; Dohi, Y. *Am J Inf Control Online* 2004, 31, 27.
4. Zhu, P.; Sun, G. *J Appl Polym Sci* 2004, 93, 1037.
5. McCarthy, B. J.; Greaves, P. H. *Wool Sci Rev* 1988, 65, 27.
6. Freddi, G.; Arai, T.; Colonna, G. M.; Boschi, A.; Tsukada, M. *J Appl Polym Sci* 2001, 82, 3513.
7. Dong, Q.; Su, H.; Zhang, D. *J Phys Chem* 2005, 109, 17429.
8. Maclaren, J. A.; Milligan, B. *Wool Science: The Chemical Reactivity of the Wool Fiber*; Science: Marrickville, Australia, 1981; p 247.
9. Park, J. S.; Kim, J. H.; Nho, Y. C.; Kwon, O. H. *J Appl Polym Sci* 1998, 69, 2213.
10. Singh, A.; Puranik, D.; Guo, Y.; Chang, E. L. *React Funct Polym* 2000, 44, 79.
11. Suslick, K. S.; Price, G. J. *Annu Rev Mater Sci* 1999, 29, 295.
12. Gedanken, A. *Ultrason Sonochem* 2004, 11, 47.
13. Landau, M. V.; Vradman, L.; Herskowitz, M.; Koltypin, Y.; Gedanken, A. *J Catal* 2001, 201, 22.
14. Perkas, N.; Wang, Y.; Koltypin, Y.; Gedanken, A.; Chandrasekaran, S. *Chem Commun* 2001, 988.
15. Salkar, R. A.; Jeevanandam, P.; Aruna, S. T.; Koltypin, Y.; Gedanken, A. *J Mater Chem* 1999, 9, 1333.
16. Pol, V. G.; Srivastava, D. N.; Palchik, O.; Palchik, V.; Slifkin, M. A.; Weiss, A. M.; Gedanken, A. *Langmuir* 2002, 18, 3352.
17. Vogell, A. I. *Textbook of Quantitative Inorganic Analysis: Theory and Practice*; Longman: London, 1962; p 256.
18. Gallico, L. *La Lana: Eventi & Progetti Elitore*; Vigliano Biellese, Italy, 2000.
19. Creighton, J. A.; Eadon, D. G. *J Chem Soc Faraday Trans* 1991, 87, 3881.
20. Carotenuto, G. *Appl Organomet Chem* 2001, 15, 344.
21. Gangopadhyay, P.; Kesavammorthy, R.; Nair, K. G. M.; Dhapani, R. *J Appl Phys* 2000, 88, 4975.
22. Volmer, M.; Stratmann, M.; Viefhaus, H. *Surf Interface Anal* 1990, 16, 278.
23. Kuzuhara A. *Biopolymers* 2005, 77, 335.
24. Pol, V. G.; Grisaru, H.; Gedanken, A. *Langmuir* 2005, 21, 3635.